Electroactive chitosan-aniline pentamer hydrogel for peripheral nerve regeneration

Deqiang MIAO, Ya LI, Zhongbing HUANG (✉), Yulin WANG, Min DENG, and Xiaohui LI

College of Biomedical Engineering, Sichuan University, Chengdu 610065, China

E-mail: zbhuang@scu.edu.cn

Supplementary materials

Synthesis of carboxyl-capped aniline pentamer (CCAP)

CCAP was synthesized according to reference with modification [22]. Briefly, 0.05 mol of N-phenyl-1, 4-phenylenediamine was reacted with 0.05 mol of succinic anhydride in dichloromethane to obtain phenyl/carboxyl-capped p-phenylenediamine. 0.01 mol of carboxyl-capped p-phenylenediamine and 0.005 mol of p-phenylenediamine in a mixture solution of dimethyl formamide (DMF) and HCl were oxidized by 0.01 mol of $(NH_4)_2S_2O_8$ at room temperature (RT) under stirring for 4 h to produce CCAP. CCAP product was washed five times with distilled water, followed by washing successively with 1,2-dichloroethane and THF in a soxhlet extractor to remove byproduct of the reactions. The product was finally dried in a vacuum oven for 24 h.

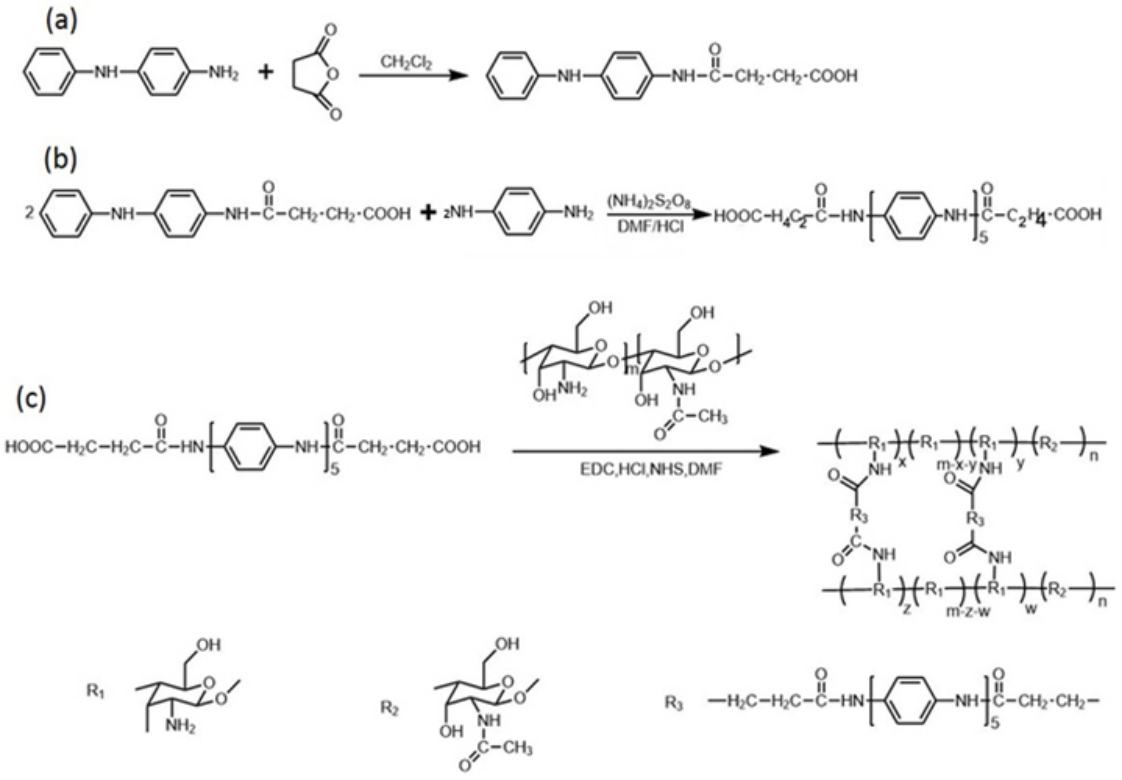

Fig. S1 Synthesis route of **(a)** phenyl/carboxyl-capped p-phenylenediamine, **(b)** carboxyl-terminated AP, and **(c)** AP-linked CS into AS-AP composites.

The contents of AP in the products were determined by UV-vis spectra. The standard curve of AP in DMSO/HCl (1 mol·L^{-1}) solution was calculated by plotting the absorbance at 308 nm for each concentration. AP content of the samples were determined by using the following formula: $C = (P/P_0) \times 100\%$, where C is the content of AP in CS-AP, P is the slope of the absorbance for the concentrations of products, and P_0 is the slope of the absorbance for the concentrations of AP, as shown in Table S1.

Table S1 AP content in the CS-AP determined by UV-Vis test

Sample	Mass of CS/g	Mass of AP/g	Fraction of AP in reaction/wt.%	Fraction of AP in sample/wt.%
CS-AP10	2	0.22	10	4.42
CS-AP15	2	0.35	15	5.68
CS-AP20	2	0.50	20	7.32

***In vitro* cytotoxicity test**

100 μL of different suspension of CS, CS-AP10, CS-AP15, and CS-AP20 (1 wt.%) was added into a 48-well plate, respectively, and the solvent was removed in a vacuum oven at 50 °C for 24 h. The plate was sterilized with 75% alcohol for 30 min, and irradiated with ultraviolet for 12 h. Then the 48-well plate was washed three times with PBS and three times with culture medium of Dulbecco's modified eagle medium (DMEM) in 30 min at 37 °C. Differentiated PC12 cells were cultured in DMEM containing 10% fetal bovine serum (FBS) at 37 °C in 5% CO_2.

The cytotoxicity of CS and CS-AP films was evaluated using Methyl Thiazolyl Tetrazolium (MTT) assay by culturing PC12 in 48-well plate, respectively. 0.5 mL of the suspension of PC12 cell (including ~10000 cells) was added into each well. After culture of 24, 48, and 72 h, respectively, 50 μL of MTT reagent (5 mg·mL^{-1}) was added into each well and the plate was incubated for 4 h protected from direct light in a constant temperature incubator. Subsequently, the supernatant in each well was carefully removed, and 0.4 mL of DMSO was added into each well. After the plate was gently shaken for 10 min, 200 μL of the upper solution from each well was transferred to a 96-well culture plate and their absorbance was measured at 480 nm on a microplate reader (VERSA max, Molecular Devices, USA).

After incubation for 24, 48, and 72 h, the living and the dead cells on CS-AP hydrogel were stained for 30 min with LIVE/DEAD® Viability/Cytotoxicity Kit, respectively. The stained cells were observed under the inverted fluorescence microscope.

Animal surgery

Sprague Dawley (SD) rats were purchased from the Laboratory Animal Center of Sichuan University (Chengdu, China). Animals were cared for within the guidelines of the Institution Animal Care and Use Committee at Sichuan University. All the experiments related to living subjects were performed in compliance with the relevant laws, ethical committee and guidelines of the Institution Animal Care and Use Committee at the Laboratory Animal Central of Sichuan University. In total, 30 male adult SD rats with an age of 2 months and a weight of (200±20) g were selected for *in vivo* experiment. They were randomly divided into five groups: CS, CS-AP10, CS-AP15, CS-AP20, and autograft groups. All animals were placed at a stable temperature with specific pathogen-free requirements. After the first week of the adaptation, these rats were intraperitoneally injected with the urethane (1.5 g·kg^{-1}) for anesthesia and the gentamicin (8.4 mg·kg^{-1}) for the anti-infection of their wound. After the hair on their incision site was removed, an incision was made on the lateral side of the left thigh to expose the sciatic nerves. The surgical

procedure was performed under a stereomicroscope. For the autografts group, a 5-mm long sciatic nerve was excised and re-implanted after inverted. For the experimental group, the sciatic nerve defect was bridged using silicone conduit with an outer diameter of 2 mm and a length of 9 mm, which was consistent with the sciatic nerve. For four groups, autograft and silicone conduits were sutured to the epineurium of nerve stumps using a 10-0 monofilament nylon suture. After the suture, the CS, CS-AP10, CS-AP15, and CS-AP20 hydrogels were carefully injected into the conduit through the suture gap using syringe with 25 gauge needles, respectively. Finally, the wounds were successively sutured with 4-0 nylon sutures and treated with iodine. All rats received the daily gentamicin injection intraperitoneally after surgery for the following two days. Observations and operations were performed at 3 and 6 weeks, respectively.

Histological analysis

First, the rats were subjected to over-dosage intraperitoneal anesthesia with urethane. For the autografts group, connective tissue coating on the regenerated nerves was carefully removed by a surgical knife blade. For the experimental group, the regenerated nerve was obtained by cutting open the external silicone tube. All regenerated samples were fixed with 4% of paraformaldehyde, embedded in resin and cut into semi-thin and ultrathin sections, respectively. Semi-thin sections were stained by HE and TB to observe them under the microscope, and the number of myelinated fibers in the middle portion of the repair nerves was counted. Ultrathin sections were stained by osmic acid, and observed with TEM to analyze the diameter of myelinated fibers and myelin thickness.

Triceps surae muscles were integrally harvested from each group, fixed with 4% paraformaldehyde to maintain their properties *in vivo* and embedded in the paraffin. Images were acquired from five random fields in each sample. The recovery state of muscle was analyzed by dividing the collagen fiber area in the total area of collagen and muscle fiber.

FT-IR spectrum of CS-AP

FT-IR spectra of CS, AP, and CS-AP20 hydrogel were shown in Fig. S2. The FT-IR spectrum of CS exhibited the adsorption peaks at 1660 and 1590 cm^{-1} assigned to the C=O stretching (amide) and the N−H bending (amine), respectively. The band at 1021 cm^{-1} was assigned to the C−O stretching vibrations of CS. In the AP pattern, the band at 1697 cm^{-1} was assigned to the absorption from the carbonyl groups in COOH, and the peaks at 1581 and 1503 cm^{-1} were attributed to vibrations of the benzene ring and the quinoid ring, respectively. Compared with the spectra of CS and AP, there were characteristic peaks at 1021 and 1660 cm^{-1} from CS in Curve c of CS-AP20, but also an absorption peak at 1498 cm^{-1} corresponding to the quinoid ring from AP. All of these results demonstrated that the CS-AP hydrogels were successfully prepared.

Young's modulus of CS and CS-AP15 films

As shown in Fig. S4, the addition of AP significantly improved the Young's modulus (from 5.02 to 6.69 MPa), indicating that AP segment crosslinked the chitosan and reinforced its mechanical strength.

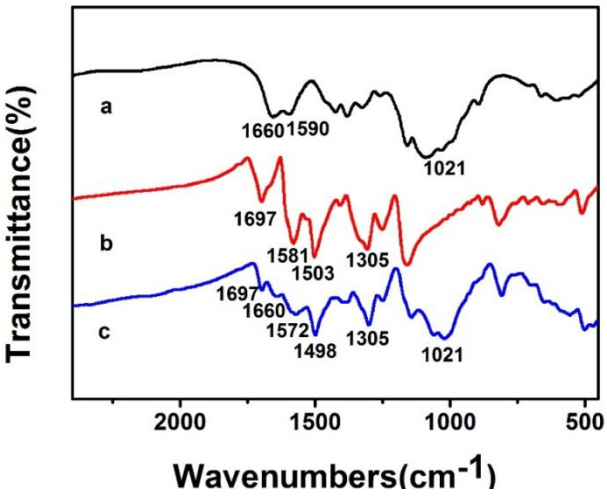

Fig. S2 FT-IR spectra of CS (a), AP (b), and CS-AP20 (c).

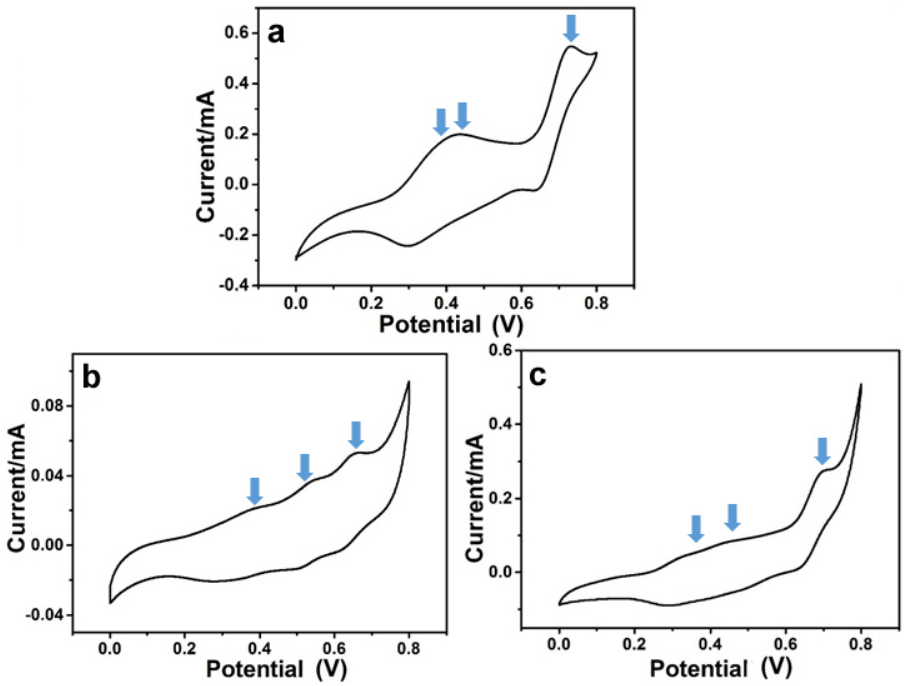

Fig. S3 Cyclic voltammograms of three samples in the mixture of DMSO and HCl: **(a)** AP; **(b)** CS-AP15; **(c)** CS-AP20.

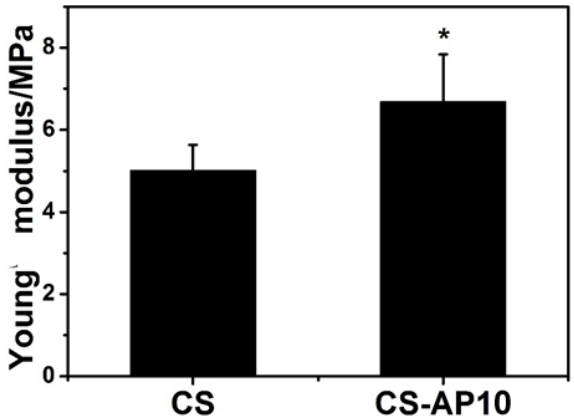

Fig. S4 Young's moduli of CS and CS-AP10 samples. All data were expressed as the mean ± SD (n = 3). *P < 0.05 shows the significant difference between two groups.

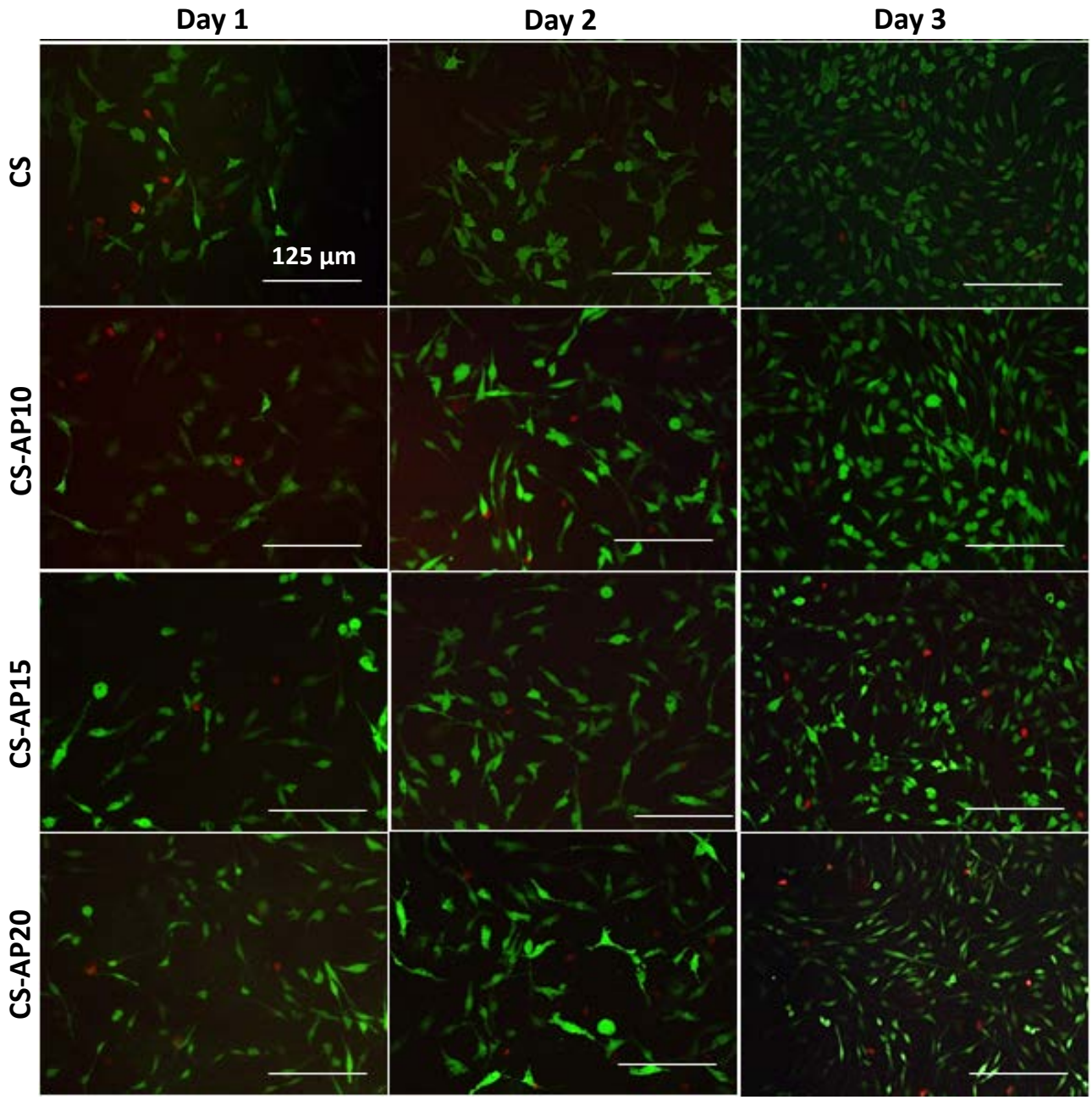

Fig. S5 Fluorescent images of PC12 cells on CS-AP hydrogels stained by live/dead assay after cell cultures for 1, 2, and 3 d, respectively.

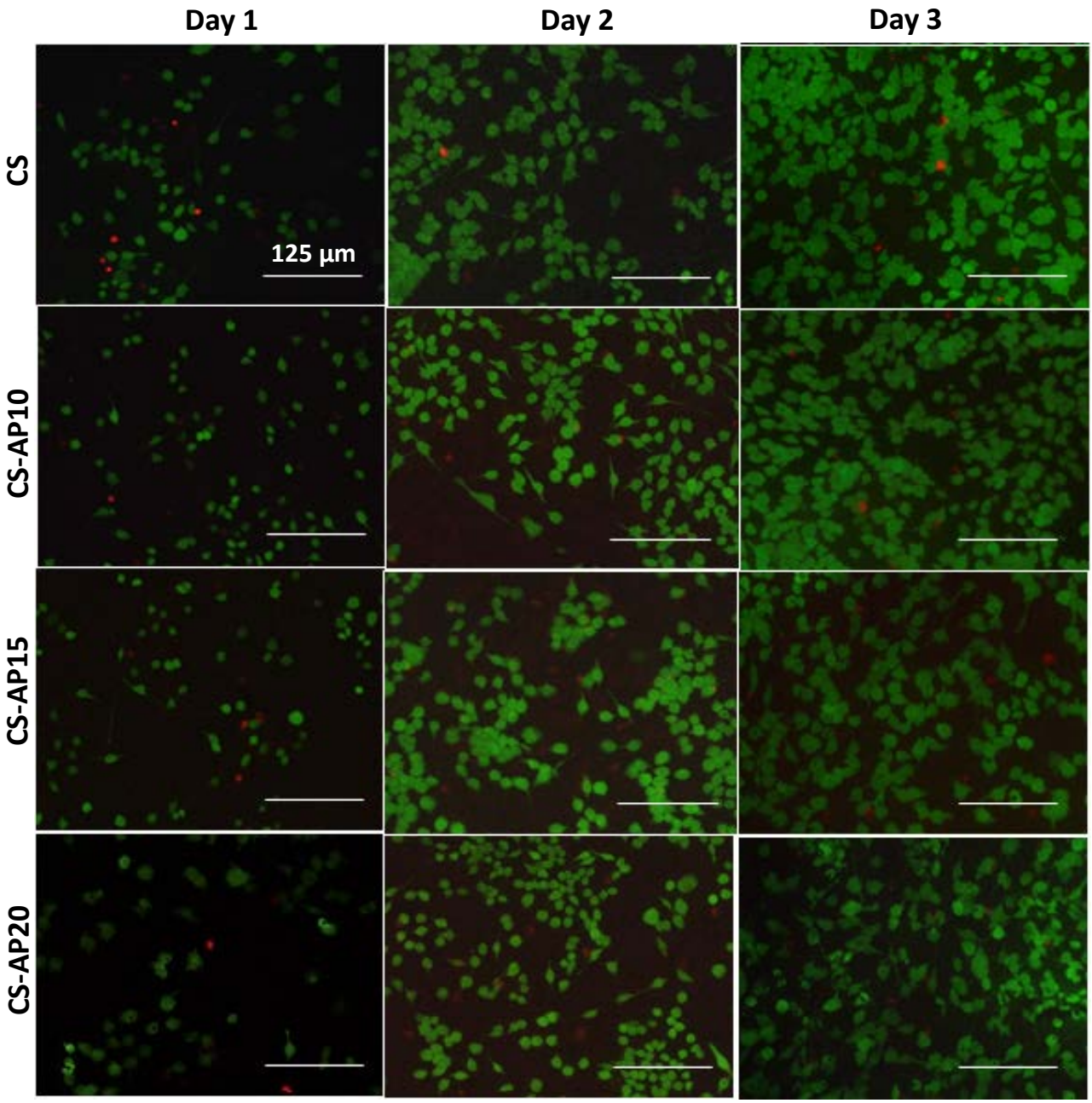

Fig. S6 Fluorescent images of RSC96 on CS-AP hydrogels stained by live/dead assay after cell cultures for 1, 2, and 3 d, respectively.

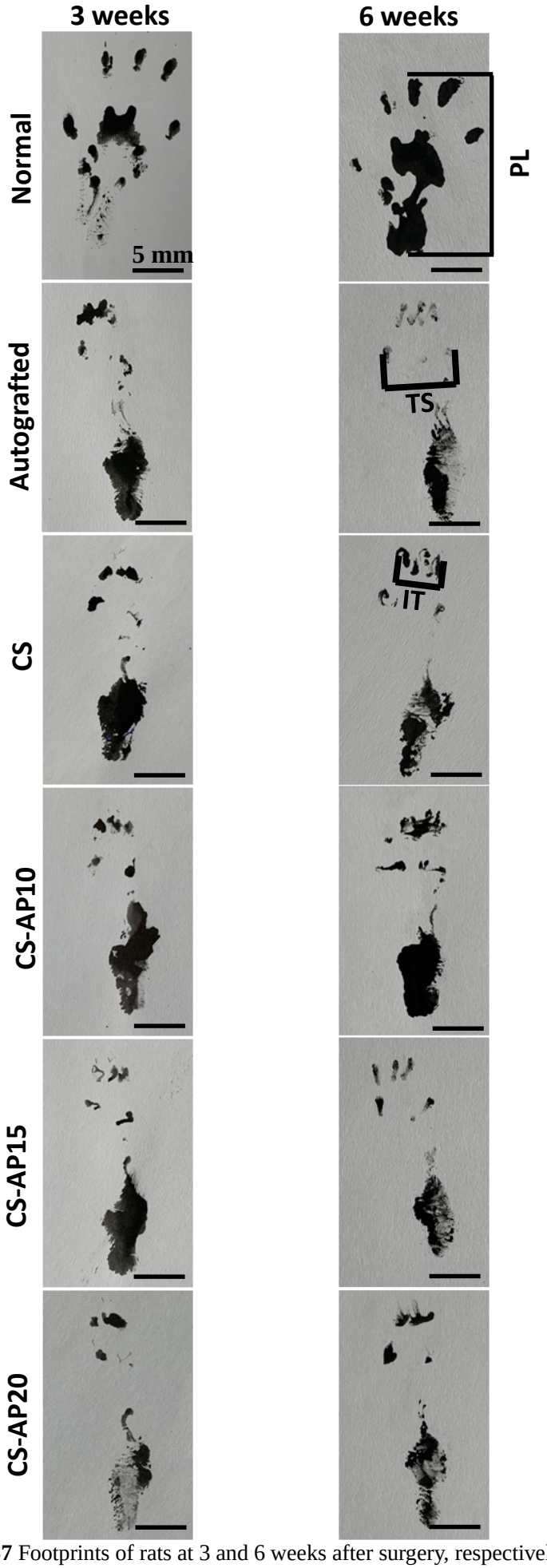

Fig. S7 Footprints of rats at 3 and 6 weeks after surgery, respectively.

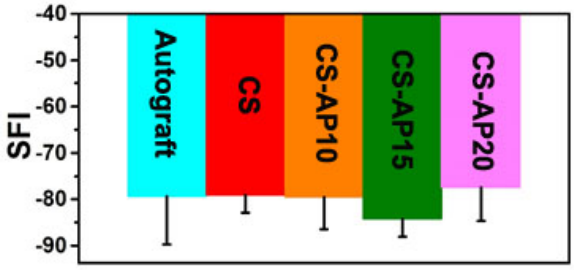

Fig. S8 SFI values of rats at 3 weeks after surgery. All data were expressed as the mean ± SD (*n* = 9).

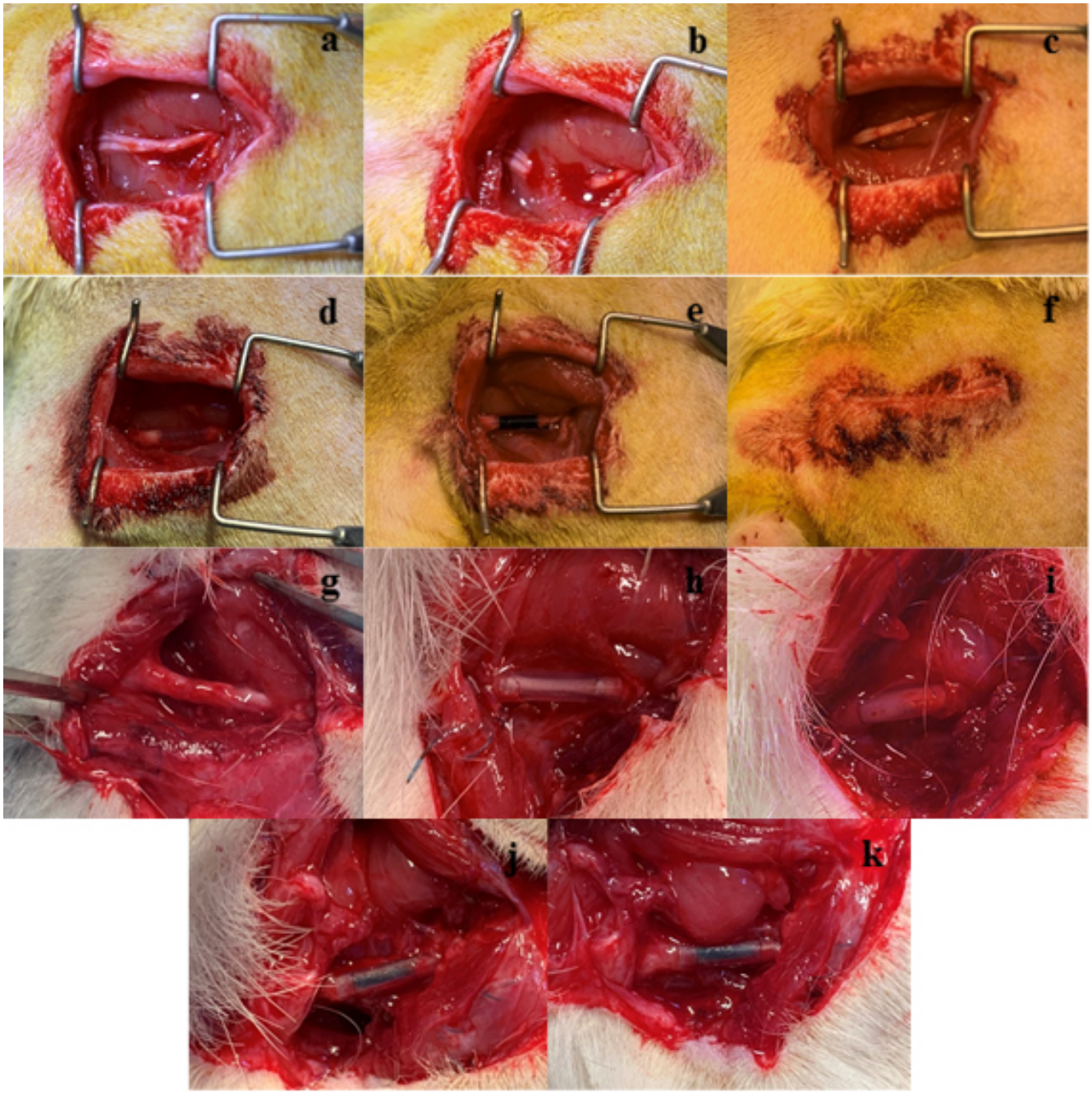

Fig. S9 The surgery procedure of implantation of CS-AP hydrogel: **(a)** the incision to expose the sciatic nerves; **(b)** the excision of 5-mm long sciatic nerve; **(c)** re-implantation of the inverted autologous nerve; **(d)** bridging silicone conduit in the site of the sciatic nerve defect; **(e)** the injection the CS-AP hydrogels; **(f)** the suture of the wounds. The surgery of the *in vivo* nerve regeneration at 6 weeks of different implanted samples: **(g)** autografted group; **(h)** CS group; **(i)** CS-AP10 group; **(j)** CS-AP15 group; **(k)** CS-AP20 group.

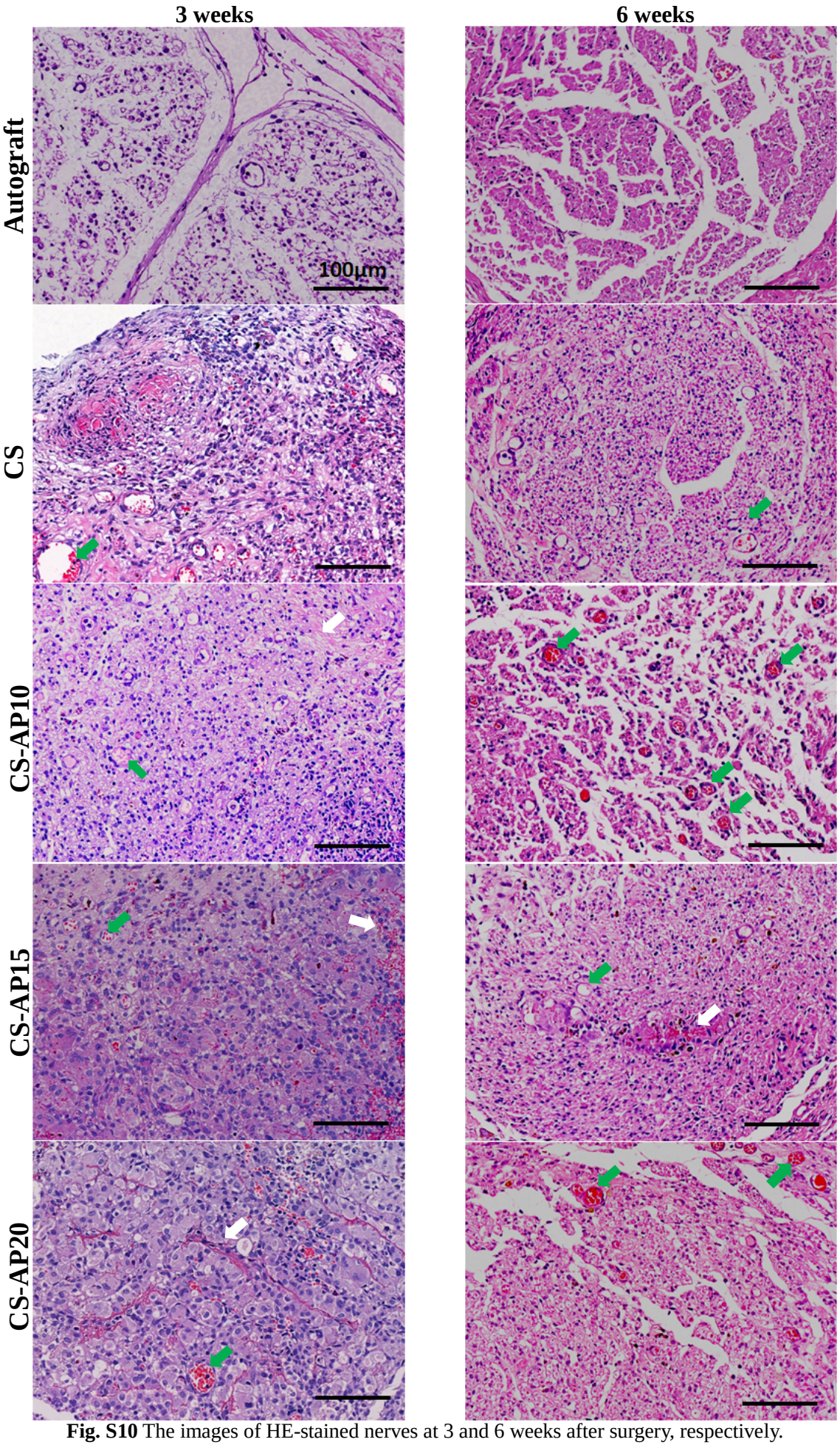

Fig. S10 The images of HE-stained nerves at 3 and 6 weeks after surgery, respectively.

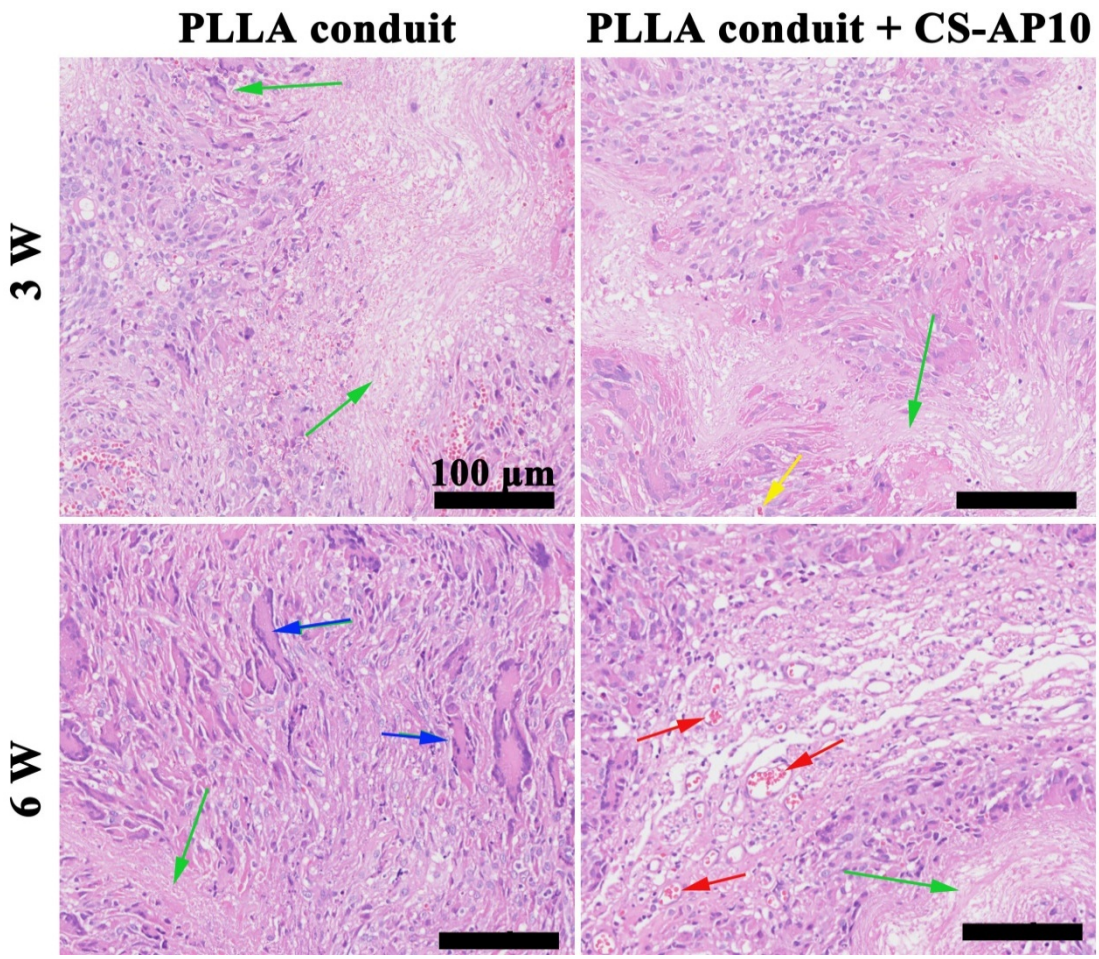

Fig. S11 Image of HE-stained nerves of PLLA conduit and PLLA + CS-AP10 at 3 and 6 weeks after surgery, respectively. Green arrows indicate the partially degraded PLLA fiber-film; and a yellow arrow indicates a slice of non-degraded CS-AP10, and a blue arrow indicates the macrophage nucleus, and red arrows indicate the new microvessels.

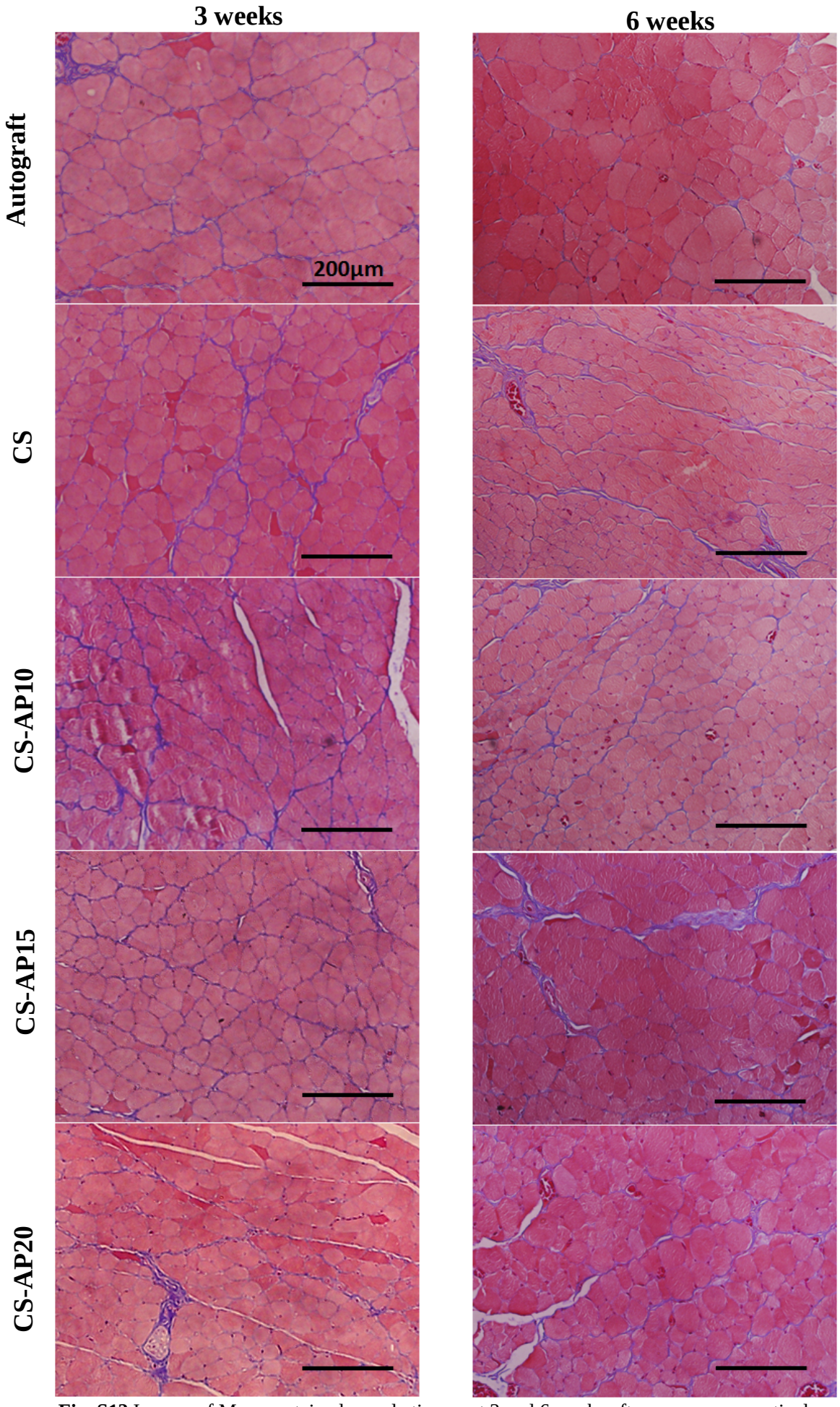

Fig. S12 Images of Masson stained muscle tissues at 3 and 6 weeks after surgery, respectively.

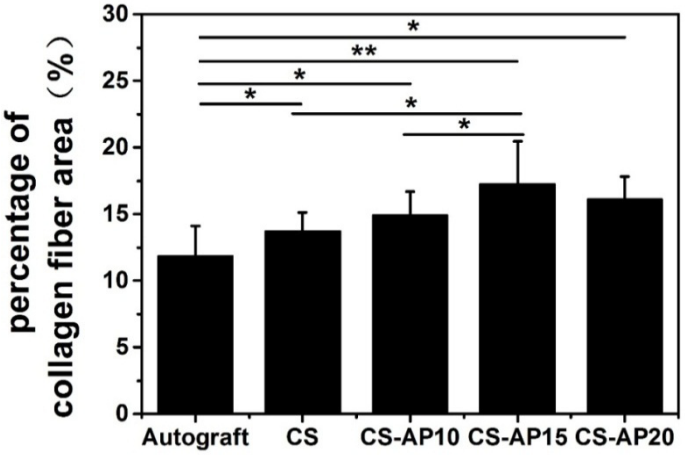

Fig. S13 Average percentage of collagen fiber area at 3 weeks after surgery. Data are expressed as the mean ± SD (n = 15). *P < 0.05; **P < 0.01.

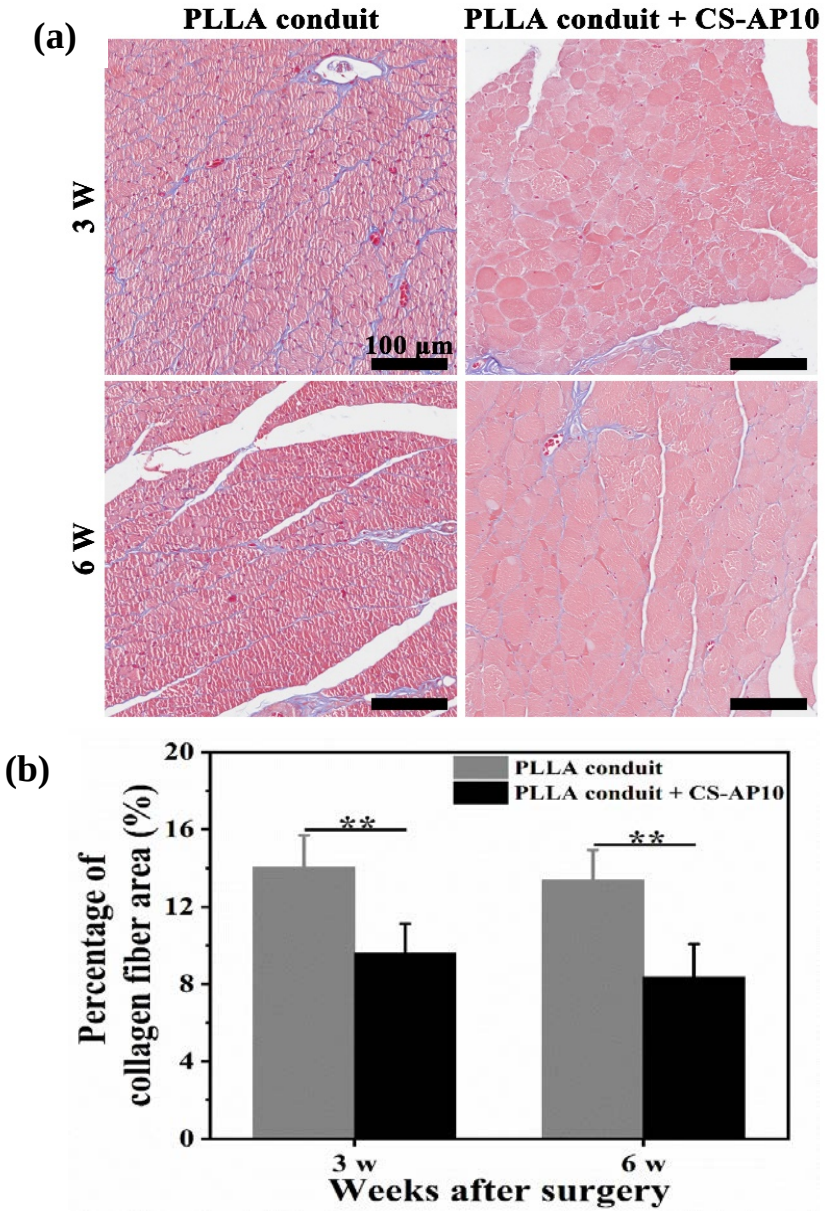

Fig. S14 The evaluation of Masson-stained muscle tissues of PLLA conduit and PLLA + CS-AP10 at 3 and 6 weeks after surgery, respectively: **(a)** images of tissue section; **(b)** percentage of collagen fiber area, **P < 0.01.

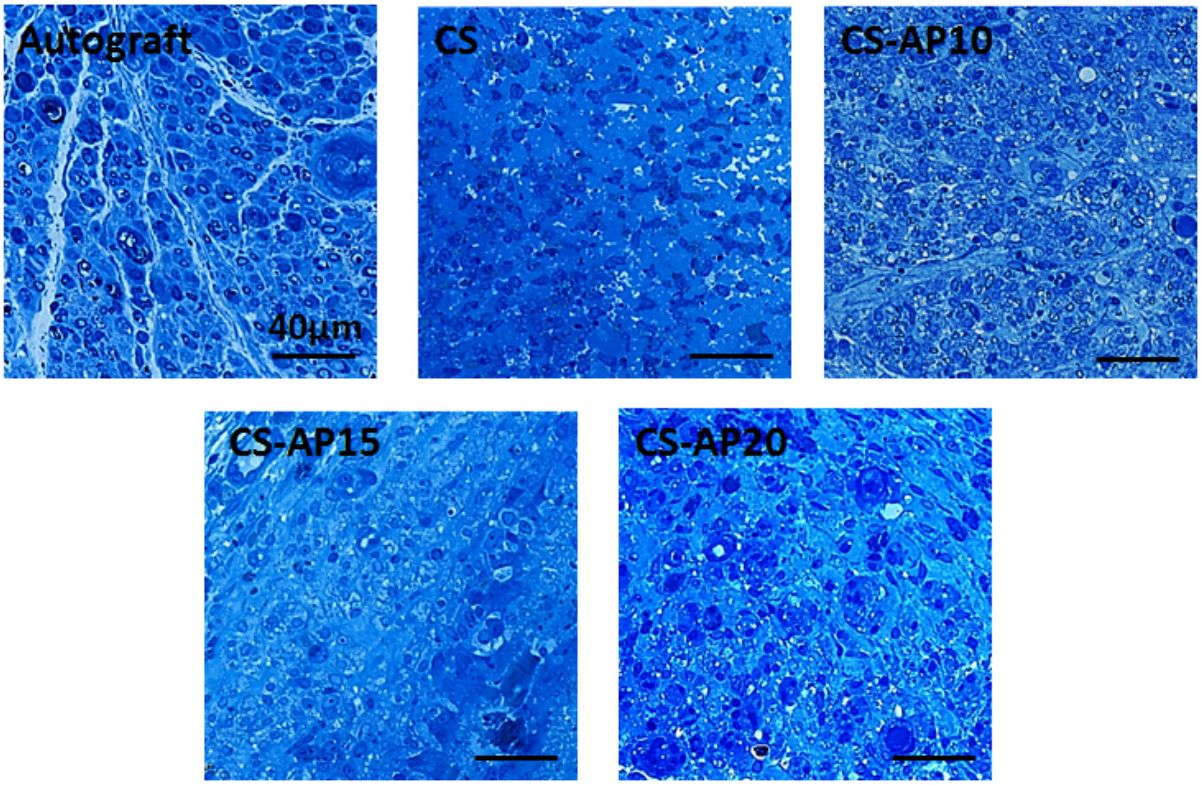

Fig. S15 Images of TB-stained nerves of different experiment groups at 3 weeks after operation.

Structure analysis of myelinated axons

The morphology and the thickness of the new myelin sheath were observed from TEM, as shown in Fig. S16. From the image of 3 weeks, the regenerated axons were distributed in bundles and tightly wrapped in myelin sheaths (shown by red arrows) in autografted group and CS-AP10 group. The myelin sheaths in autografted group were thick and tight, while those in CS-AP10 were thin with loose lamellar structure. In the other groups, there were basically regenerated bare axons (shown by green arrows) and very few myelin sheaths with disordered structure.

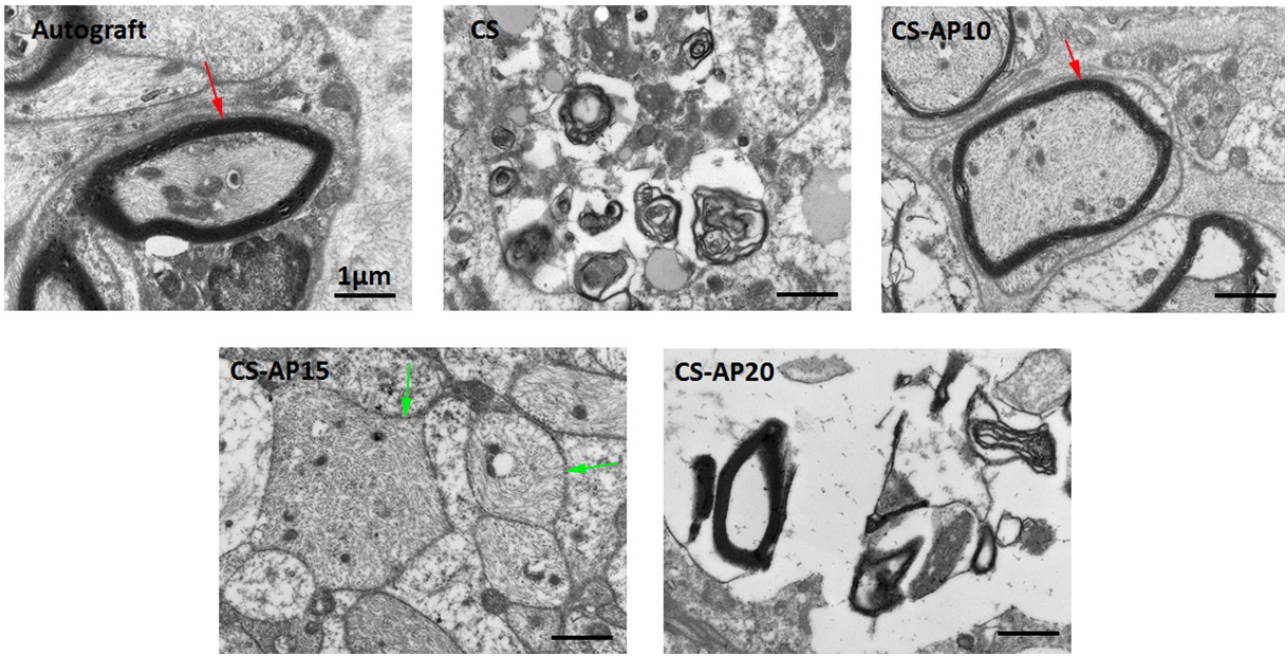

Fig. S16 TEM images of ultra-sections of myelinated axons of different groups at 3 weeks of post-operation.

Immunofluorescence analysis of regenerated nerves

To further verify the promoting effect of the CS-AP on nerve regeneration, regenerated nerve tissues at 3 weeks and 6 weeks after surgery was analyzed with immunofluorescence assay and their results were shown in Figs. S17 and S18. DAPI with blue fluorescence represented cell nucleus. Neurofilament 200 (NF200) with green fluorescence represented an important sign of regenerated mature axon. S100 (acid calcium-binding protein) with red fluorescence represented migration and proliferation of Schwann cells which played a neurotrophic role. As shown in Fig. S17, the fluorescence signal in the autografted group was orderly, clear and was more punctate in distribution, while those in experimental groups were distributed in continuous patches, suggesting that the experimental group had not yet formed regular nerve fibers in 3 weeks after surgery. And in experimental groups, the red fluorescence distribution was scattered and the blue fluorescence signal increased, which was caused by the aggregation of Schwann cells and macrophage, indicating that the nerve regeneration was under way, and tissue repair process was in the myelination stage. At 6 weeks, the number of macrophage nucleus (blue dots) decreased, due to reducing inflammatory response. As shown in Fig. S18, there was an area surrounded by a blue nucleus filled with green fluorescence (shown by white arrow), demonstrating that micro-vessels in CS-AP10 group were formed, guiding the growth of nerves and delivering nutrients.

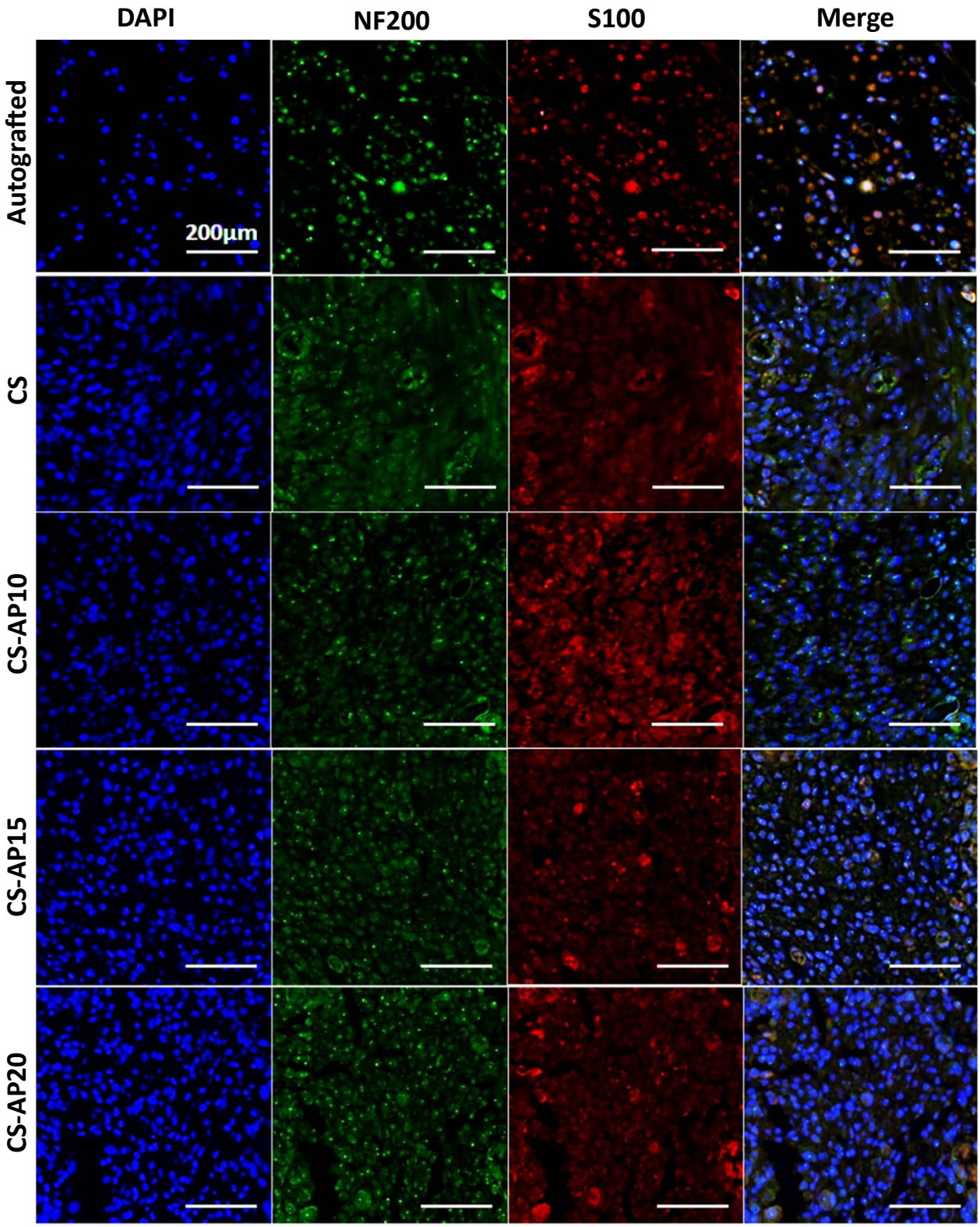

Fig. S17 Images of immunofluorescent staining for NF200 and S100 of different groups at 3 weeks after operation.

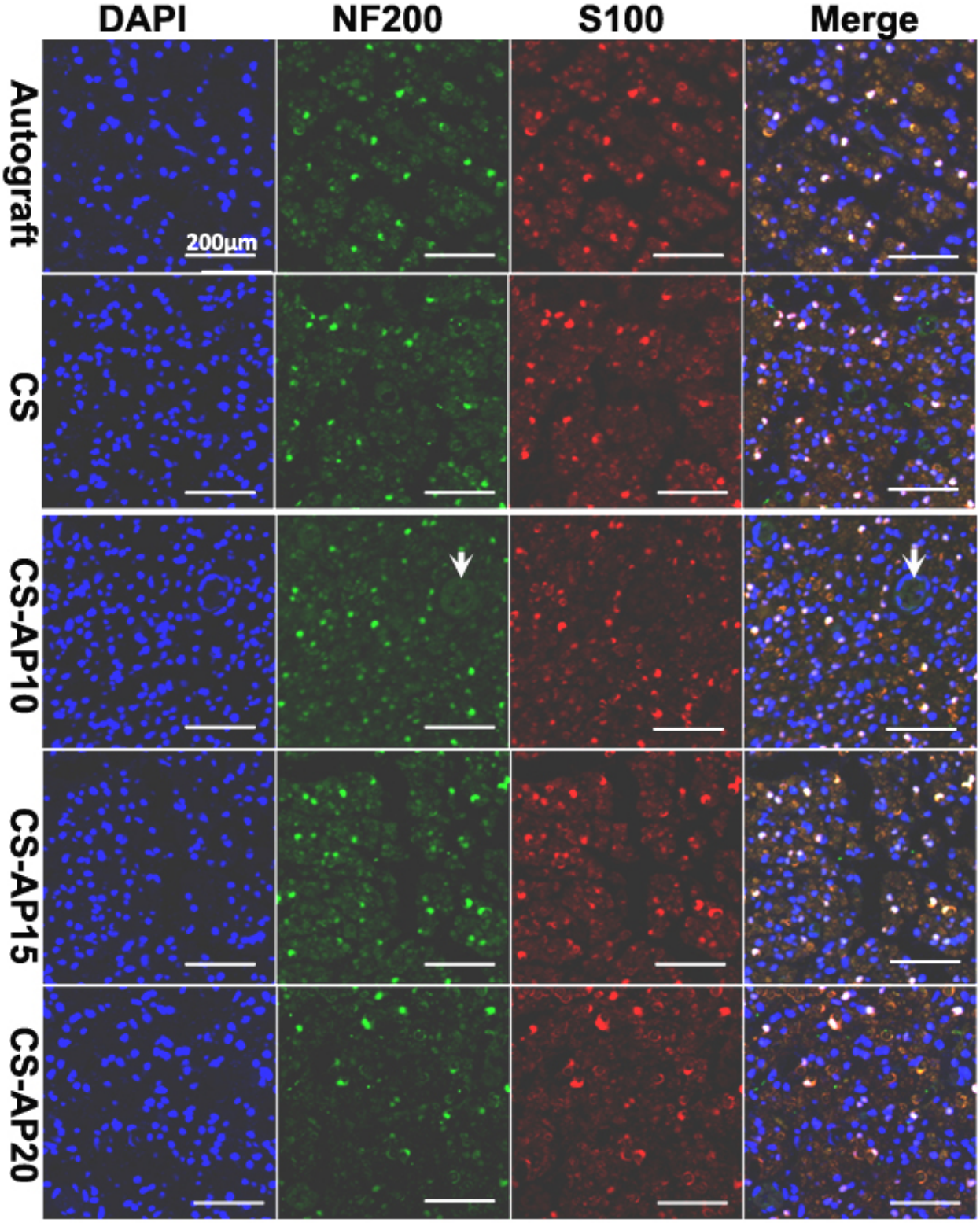

Fig. S18 Images of immunofluorescent staining for NF200 and S100 of different groups at 6 weeks after operation.